

3. Amundsen-Scott South Pole Station (9/14/20–3/28/21)

The 2020–2021 data season at Amundsen-Scott South Pole Station includes the period 9/14/20 to 3/28/21. This season was affected by the COVID-19 pandemic and no site visit took place during this period. The system performed without significant problems, although its wavelength stability was degraded, requiring frequent adjustment of the system’s wavelength registration during post-processing.

A total of 17,606 SUV-100 spectra were assigned to Volume 30.

Like for the previous three seasons, measurements of the 320 nm channel of the GUV-541 radiometer (S/N 29239) that is installed next to the SUV-100 spectroradiometer drifted greatly. GUV data products had to be produced without utilizing measurements of this channel. A comparison of calibrated GUV and SUV data performed during the Volume 26 season indicated that the quality of GUV data products is only marginally affected by the omission of the 320 nm channel. Solar data of the GUV are therefore part of the published datasets.

The system’s PSP radiometer was installed during the site visit in January 2020. Its serial number is 27228F3 and it has a calibration factor of $8.332 \times 10^{-6} \text{ V}/(\text{W m}^{-2})$.

3.1. Irradiance Calibration

The on-site irradiance standards used for calibrating the SUV-100 spectroradiometer during the reporting period were the lamps M-666, 200W021, 200W013, 200WN005 and 200WN006. Lamps M-666, 200W021, and 200W013 are “working standards” that are used on a regular basis. Please see previous Operations Reports on the history of these lamps. Lamps 200WN005 and 200WN006 were left at the South Pole in March 2014. Both lamps are designated “long-term” standards and are typically only used during site visits. Both lamps were calibrated by CUCF in August 2013 (see below).

Comparisons of calibrations with the various lamps suggested that the brightness of lamp 200W013 fluctuated by about 1% over the season. Similar fluctuations have been observed also during the last season. Hence absolute scans of the lamp were not used for the preparation of solar data.

Calibration history of long-term standards

The long-term standards 200WN005 and 200WN006 were calibrated against lamps 200WN001 and 200WN002 on 8/20/13. Lamps 200WN001 and 200WN002 had in turn been calibrated by Biospherical Instruments in November 2012 against the NIST standard F-616 using a multi-filter transfer radiometer. NIST standard F-616 is traceable to the detector-based scale of irradiance established by NIST in 2000. At the time lamps 200WN001 and 200WN002 were calibrated, they were also compared with the long-term traveling standard 200W017 of the NSF UV monitoring network. The irradiance scales of NIST standard F-616 and lamp 200W017 agreed to within 0.3%.

In early 2020, the chain of calibrations applied to solar data of the NSF and NOAA monitoring networks between 1996 and 2019 was re-evaluated (Bernhard and Stierle, 2020). This analysis suggested that the scale of spectral irradiance of NIST standard F-616 is low compared to the scale of primary standards used before 2013. This bias ranges between –2% at 300 nm, –1% at 375 nm, and less than $\pm 0.5\%$ between 420 and 600 nm. **Version 2 solar data of Volume 29 were scaled upward accordingly, however, Version 0 remain traceable to the original scale of the primary standard F-616.**

Figure 3.1. shows a comparison of lamps M-666, 200W021, and 200WN006 based absolute scans performed on 10 September 2020, shortly before the commencement of the solar data season at the South Pole. The scales of spectral irradiance of the working standards M-666 and 200W021 agree with that of the

long-term standard 200WN006 to better than $\pm 0.5\%$ on average. A comparison of the three working standards near the end of the season, on 3/26/21, resulted in a similarly good agreement.

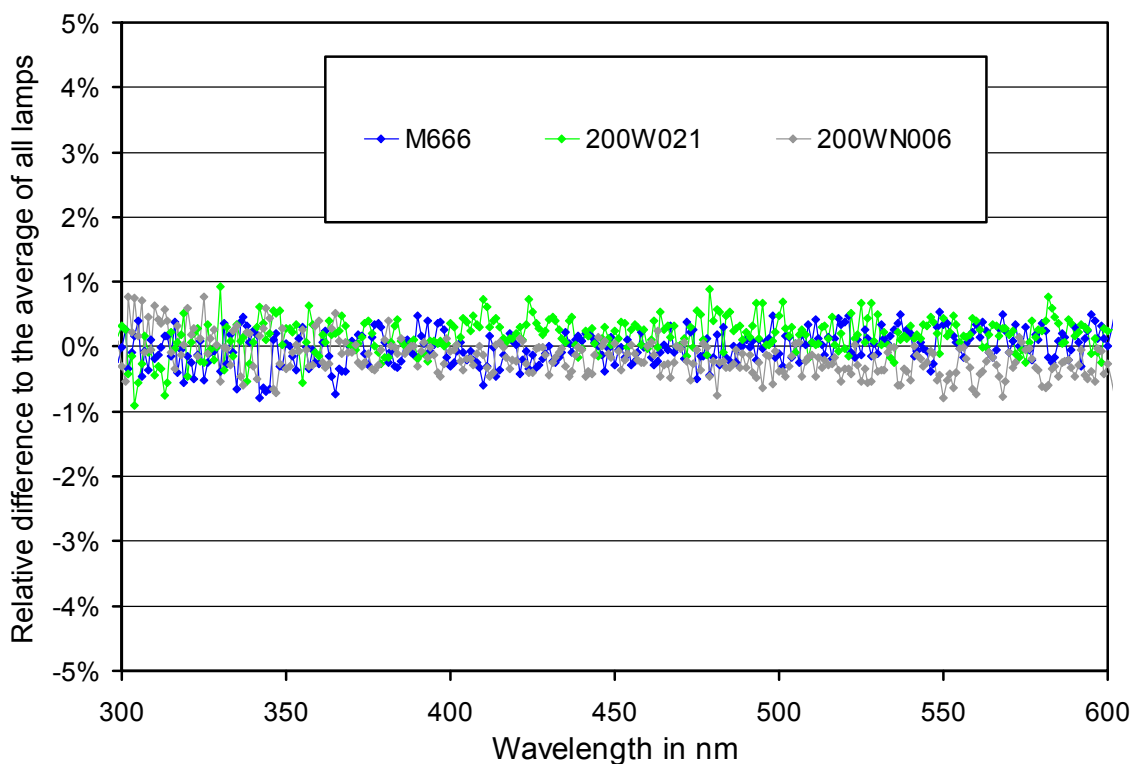


Figure 3.1. Comparison of South Pole lamps M-666, 200W021, and 200WN006 based absolute scans performed on 10 September 2020.

The GUV-541 radiometers was calibrated vicariously against SUV-100 Version 0 data. Calibration factors were established in the same way when data of previous volumes were processed. Calibration factors of the last six years (Volumes 23 –30) agree to within $\pm 1.5\%$ ($\pm 1\sigma$) for all GUV channels, with exception of the drifting 320 nm channel. This result confirms the good consistency of calibrations over time.

3.2. Instrument Stability

The temporal stability of the spectroradiometer’s sensitivity was assessed with (1) bi-weekly calibrations utilizing the on-site standards, (2) daily “response” scans of the internal irradiance reference lamp, (3) comparison with data of the collocated GUV-541 radiometer, and (iv) model calculations, which are part of “Version 2” data edition.

The internal reference lamp is monitored with a filtered photodiode with sensitivity in the UV-A, called “TSI”. This photodiode has proven to be very stable over time and its measurements therefore allow to decouple temporal drifts of the internal lamp from changes in the SUV-100’s responsivity. These changes may be caused by variations in monochromator throughput or PMT sensitivity. Figure 3.2 shows changes in TSI readings and PMT currents at 300 and 400 nm, which were derived from the daily scans of the internal lamp during the reporting period. TSI measurements steadily decreased by about 2.5% during the reporting period, indicating some dimming of the internal reference lamp. PMT currents at 300 and 400 nm also showed a downward trend in response to the change in the lamp’s output but their variability is larger than that of the TSI data. In addition, there is sudden drop in both currents of about 4% on 11/26/20 when the “Spectralink” unit, which controls monochromator and PMT high-voltage, had to be rebooted. It is

unknown why this reboot led to decrease in the PMT’s sensitivity. However, the magnitude of these variations is within the normal range observed in previous years. The resulting changes in the instrument’s sensitivity were corrected by adjusting the system’s calibration as described below.

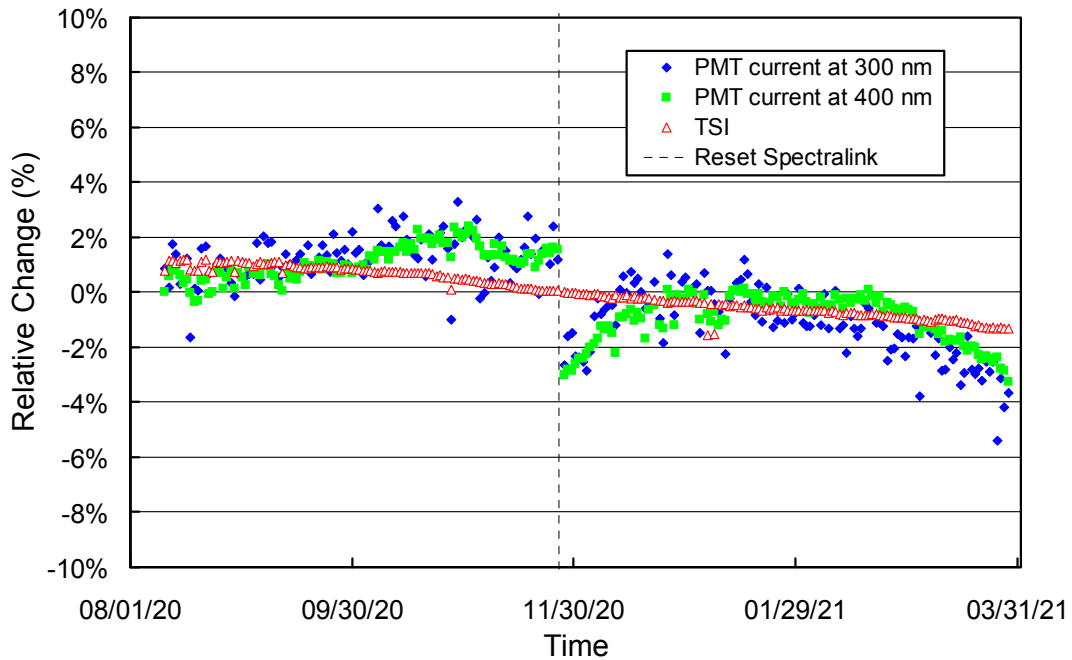


Figure 3.2. Time-series of PMT current at 300 and 400 nm, plus the TSI signal, derived from daily measurements of the SUV-100’s internal irradiance standard. Data are normalized to the average of the whole period.

A comparison of GUV-541 and SUV-100 measurements allows to detect anomalies in SUV-100 data. Accordingly, Figure 3.3 shows the ratio of GUV-541 (340 nm channel) and SUV-100 measurements. The latter were weighted with the spectral response function of the GUV’s 340 nm channel. The ratio was normalized to its average and should ideally be equal to one at all times. The graphs indicates that GUV and SUV measurements are generally consistent to within $\pm 4\%$. The few outliers, in particular during Period P2, can be explained by shading from obstacles (e.g. air sampling masts) that are in the field of view of the instruments. Because GUV and SUV radiometers are not positioned at exactly the same location, the shadows from these obstacles fall on the collectors of the two instruments at different times. Scans affected by shading from stacks were flagged in the SUV-100 Version 2 dataset, removed from the GUV dataset, but remain part of the SUV-100 Version 0 dataset.

Three calibration functions were applied to SUV-100 data of the reporting period. Times when the calibration changed are indicated by vertical lines in Figure 3.3. More information on these calibrations is provided in Table 3.1. Figures 3.4 shows ratios of calibration functions relative to the function applied during the first period (Period P1).

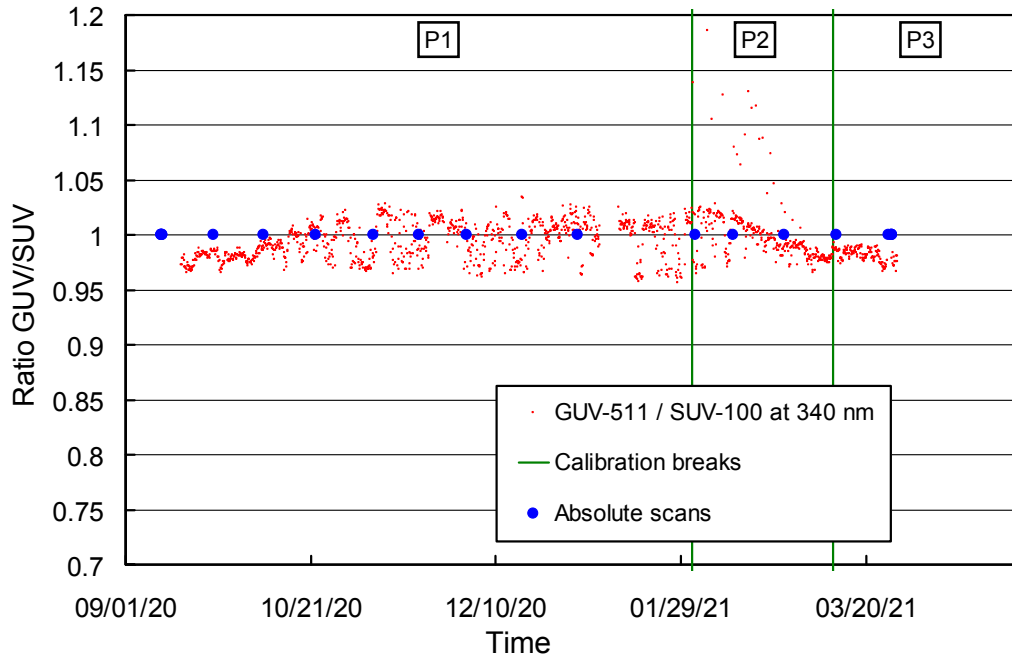


Figure 3.3. Ratio of GUV-541 (S/N 29239) measurements (340 nm channel) with SUV-100 measurements. SUV-100 data were weighted with the spectral response function of this GUV channel. The vertical green lines indicate times when the calibration applied to SUV-100 data was changed (see also Table 3.1).

Table 3.1 Calibration periods for South Pole data of Volume 30.

Period	Period range	Number of absolute scans
P1	06/02/20 – 01/31/21	10
P2	02/01/21 – 03/10/21	2
P3	03/11/21 – 06/20/21	3

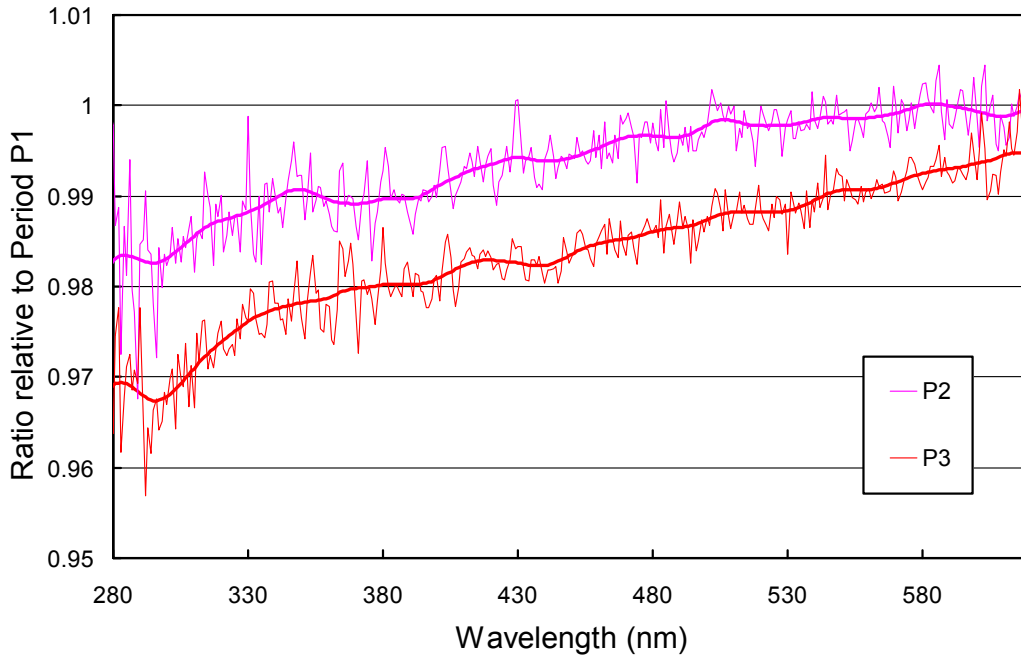


Figure 3.4. Ratios of spectral irradiance assigned to the internal lamp relative to the spectral irradiance of Period P2. Thin lines indicate the actual ratio; thick lines indicate smoothed ratios. Calibration functions are based on the latter.

3.3. Wavelength Calibration

The wavelength stability of the system was monitored with the internal mercury lamp. Information from the daily wavelength scans was used to homogenize the data set by correcting day-to-day fluctuations in the wavelength offset. The wavelength-dependent bias of this homogenized dataset and the correct wavelength scale was determined with the Version 2 Fraunhofer line correlation method (Bernhard et al., 2004). The resulting correction function is shown in Figure 3.5.

Figure 3.6 indicates the wavelength accuracy of Version 0 data for five wavelengths in the UV and visible range. The plot was generated by applying the Version 2 Fraunhofer-line correlation method to the corrected data. Residual wavelength shifts are typically smaller than ± 0.15 nm, but there is still a considerable day-to-day variability. The wavelength accuracy was further improved when processing Version 2 data by breaking the dataset into 77 periods and calculating separate correction functions for each period. Figure 3.7 indicates the wavelength accuracy of Version 2 data. A significant improvement in the wavelength uncertainty can be observed when comparing Figs. 3.6 and 3.7. The standard deviation of the residual wavelength shifts is smaller than 0.032 nm at all wavelengths.

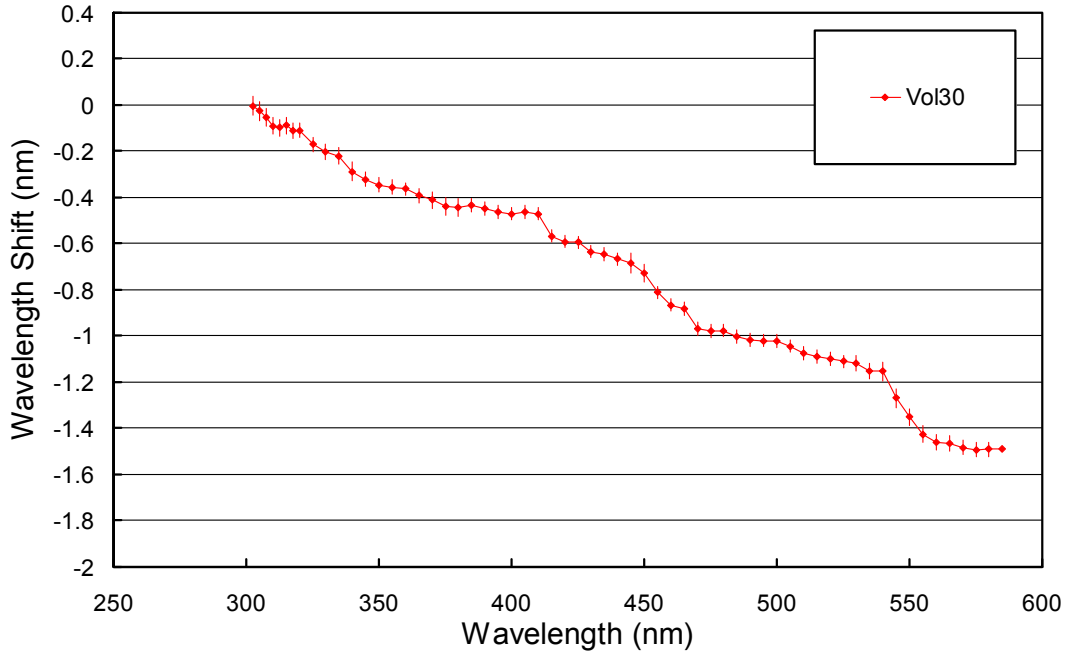


Figure 3.5. Monochromator non-linearity correction functions.

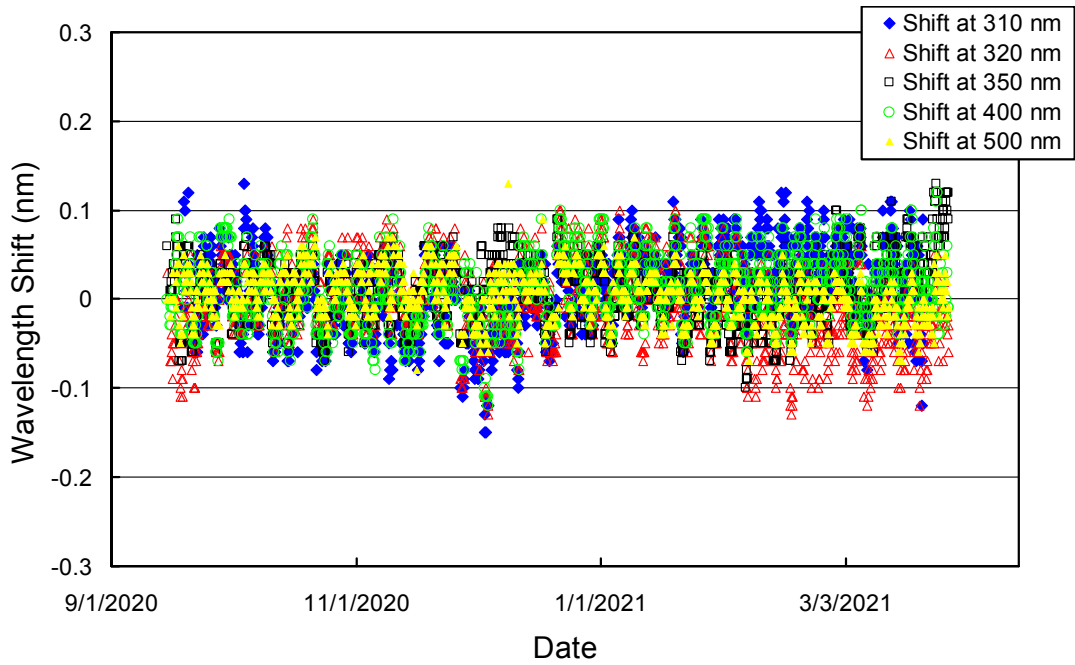


Figure 3.6. Wavelength accuracy check of Version 0 data at five wavelengths by means of Fraunhofer-line correlation.

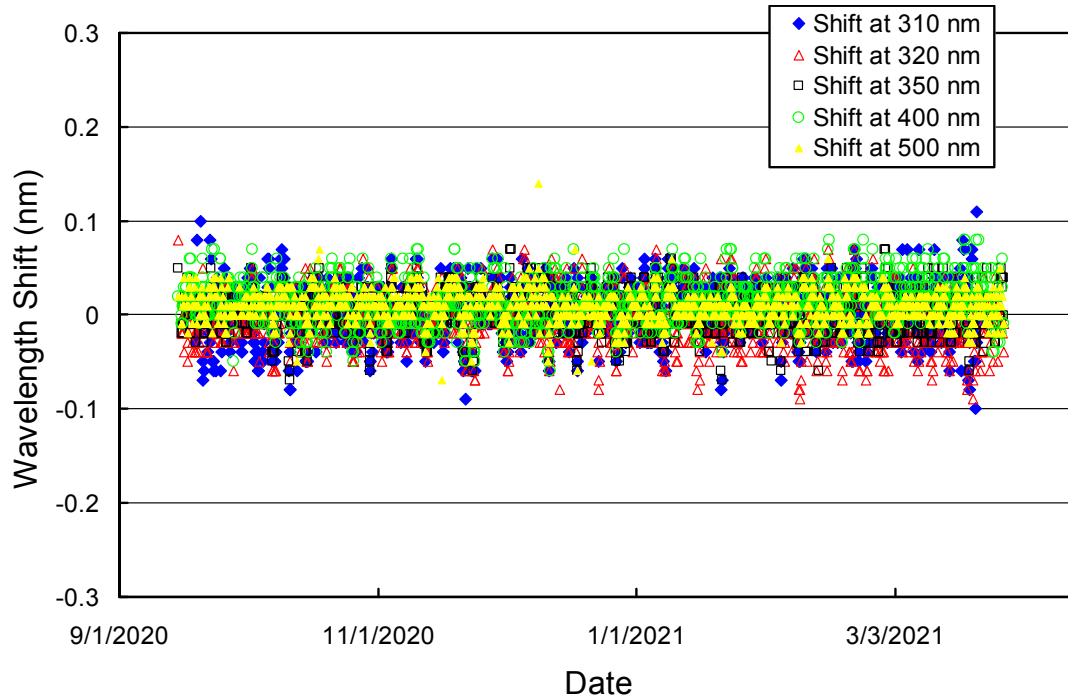


Figure 3.7. Wavelength accuracy check of Version 2 data at five wavelengths by means of Fraunhofer-line correlation.

References

Bernhard, G., C. R. Booth, and J. C. Ehranjian. (2004). Version 2 data of the National Science Foundation’s Ultraviolet Radiation Monitoring Network: South Pole, *J. Geophys. Res.*, 109, D21207, doi: <https://doi.org/10.1029/2004JD004937>.

Bernhard G. and S. Stierle (2020). Trends of UV Radiation in Antarctica, *Atmosphere*, 11(8), 795, doi: <https://doi.org/10.3390/atmos11080795>.